Piezoelectric Deflection Sensor for a Bi-Bellows Actuator

Yoel Shapiro, Alon Wolf, and Gábor Kósa

***Abstract*—We employ a piezoelectric transducer polyvinylidene fluoride (PVDF) for a new application: tracking the shape of a highly flexible cantilever. The sensor was attached to the bi-bellows, a pneumatic actuator developed by the authors. We demonstrate how the sensor responds to changes of the actuator's shape and discuss its limitations. The combination of an internal pressure sensor and a PVDF sensor enables measurements of external forces applied on the actuator, in addition to its self position.**

***Index Terms*—Cantilever shape measurement, data fusion, piezoelectric transducer, pneumatic actuators, sensor integration.**

I. Introduction

Compliant mechanisms have drawn increasing attention in the past few years, especially in the field of hyperredundant continuum manipulators [1]–[8]. Flexibility can be advantageous in several scenarios. For example, medical catheters sometimes perforate blood vessels during minimal invasive surgery, a hazard that could be avoided by using malleable instruments [9]. Safety considerations are a crucial consideration for any application where robots interact with humans or operate in close proximity to them, such as physiotherapeutic training or homecare robots. Furthermore, manipulator compliance increases adaptability, e.g., for search-and-rescue robots exploring rugged terrain or in grasping tasks [10], [11]. However, flexible manipulators pose a challenge: how can one accurately control a nonrigid mechanism, which bends under external loads and is deflected by obstacles?

In our previous work, we presented a single-degree of freedom (DOF) bending fluidic actuator, the bi-bellow [12] (similar works [13], [14]). As for any compliant actuator, the bi-bellows' shape cannot be monitored only by tracking the actuation variable (pressure), because of the actuator's susceptibility to external loads and constraints. Additional sensing capabilities are necessary to control the configuration of compliant actuators. Embedded sensors, such as strain sensors, cannot be occluded and are relatively resilient to changes of environmental conditions. According to our previous work [12], in order for a strain sensor to monitor a bending actuator, such as the bi-bellows, without influencing the strain field, the sensor would have to bend easily, have a large working range (up to 10% strain) and be suitable for low frequencies (<10 Hz). Traditional strain gauges do not suit this task, but novel polymeric sensors suggest a new avenue for large-strain measurements [15]–[17], some of which are commercially available [18]. In fact, we are not interested in strain per se but in deflection. For this purpose we examined polyvinylidene fluoride (PVDF), setting out to develop a large-range deflection sensor from PVDF film. In this study, we will present our endeavors to monitor deflection with a PVDF-film sensor, discuss its applicability and use our experience to show some of its advantages and shortcomings.

Manuscript received April 18, 2012; revised May 24, 2012 and August 8, 2012; accepted September 5, 2012. Date of publication September 28, 2012; date of current version January 18, 2013. Recommended by Technical Editor G. Schitter. This paper was presented in part at the 2012 IEEE International Conference on Biomedical Robotics and Biomechatronics, Rome, Italy, June 24–27.

Y. Shapiro and A. Wolf are with the Technion-Israel Institute Technology, Haifa 3200, Israel (e-mail: yoelsh@technion.ac.il; alonw@technion.ac.il).

G. Kósa is with Tel-Aviv University, Tel-Aviv 69978, Israel (e-mail: gkosa@post.tau.ac.il).

This paper has supplementary downloadable material available at http://ieeexplore.ieee.org provided by the author. The material consists of two movies depicting the actuator working at two different working ranges (0.6 bar $\sim$ 90 degrees bending, 1 bar $\sim$ 160 degrees bending). The PVDF signal is overlayed at the top of the screen, to give the reader a better understanding of the PVDF's relation to the actuator's geometry. The size of each movie is 10.6 MB, and they can be viewed with standard video players. Contact yoelsh@technion.ac.il for further questions about this work.

Color versions of one or more of the figures in this paper are available online at http://ieeexplore.ieee.org.

Digital Object Identifier 10.1109/TMECH.2012.2218115

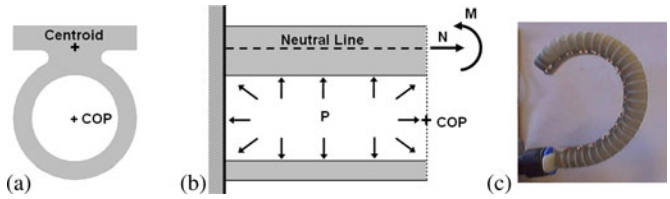

Fig. 1. Bending induced by the cross section's nonaxisymmetric profile. (a) Illustration of a cross section with its compound-beam centroid ($\bar{x}$) and the COP. (b) Side view demonstrating the equivalent tensile force N and bending moment M induced by the actuation pressure. (c) Resulting deflection of the bi-bellows actuator.

PVDF is a piezoelectric polymer, commercially available as very thin sheets (<0.1 mm), yielding easily to bending. common applications of PVDF film include various force sensors (e.g., electronic piano keys, traffic sensors, and perimeter security cables), vibration/acceleration sensors (motion/theft sensors), high-frequency resonators (ultrasound), biomedical devices [19], and many more. Typically, PVDF film has a very low capacitance (1 nF/cm^2); in order to use it as a low-frequency strain sensor, appropriate signal conditioning [20] must be applied and specialized amplifiers must be chosen. For more details on PVDF film sensors [21].

Several researchers have employed PVDF films as force or strain sensors in robotic applications; for example, Liu *et al.* embedded PVDF strips into a crawling inch-worm robot and were able to detect external contacts and internally induced contractions [22]. The work of Chen *et al.* on a bending actuator [23] is closer to our focus of attention, despite it being far less compliant than bi-bellows. They monitored deflection using PVDF strips and were able to estimate the penetration force of a needle into a soap bubble (<15 μN). Suzumori's group developed several fluidic bellow actuators with relatively elaborate structures [5], [24]. Members of this research center, Yamamoto *et al.* [25] also constructed a displacement sensor upon a 3-DOF flexible microactuator by depositing a unique PVDF paste between two electrodes. This exceedingly flexible solution allowed measuring strain on the actuator side opposite to the bending direction, where longitude strain is the greatest. The PVDF film we examined does not stretch as much as Yamamoto's sensor but, since bi-bellows is a single-DOF actuator, one side is always toward the center and the other is always toward the circumference. Embedding the PVDF sensor on the shorter (central) side might even serve to increase asymmetry and enhance bending.

In this letter, we explore the possibility of monitoring the shape of a flexible beam with a PVDF strip. We compare the PVDF signal to the pressure reading and geometric features of the bi-bellows, which are extracted via visual tracking.

II. Theory

The bi-bellows consists of a pliant body that bends when internal pressure is increased and rigid hoops that resist swelling (Fig. 3). The body's cross section is not axisymmetric. In other words, the body's centroid and the center of pressure (COP) are slightly removed from each other as shown in Fig. 1(a). The actuation pressure applies a tensile force N through the COP, equivalent to a tensile force N through the

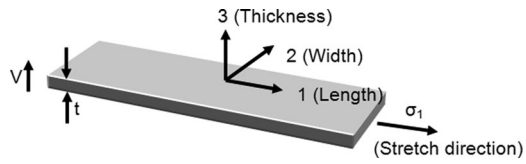

Fig. 2. Notation for a PVDF-film transducer.

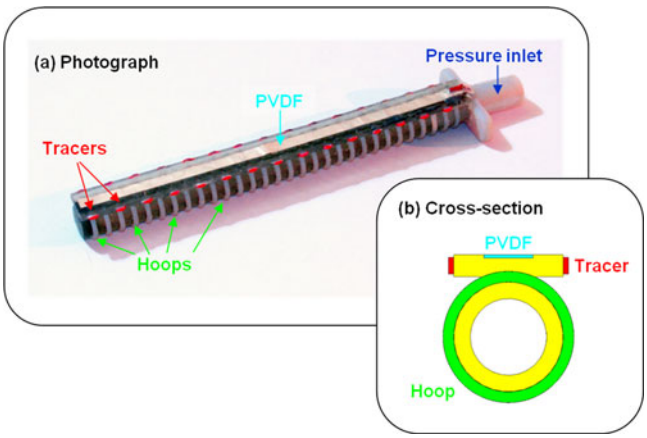

Fig. 3. Bi-bellows structure: (a) photograph and (b) cross section The Rigid hoops prevent swelling and the tracers allow visual tracking. The actuator's pliant body appears yellow in the cross section.

centroid, accompanied by a bending moment M as shown in Fig. 1(b). Internal reactions are dictated not only by the actuation pressure, but also by external forces such as the actuator's own weight, the weight of a payload, or the interaction with an obstacle (demonstrated in [12]).

Beam deflection is accompanied by a strain field growing from the centroid linearly across the cross section, the magnitude being proportional to the local curvature k. Ideally, the PVDF strip undergoes the same strain as the plane it is fixed to, at the bottom of the actuator. Strain and curvature are directly related to the beam's geometry, unlike the pressure reading. When a PVDF-film sensor is stretched (direction 1 in Fig. 2), an electric potential V builds up between its electrodes (direction 3) according to which $V = g_{31} \cdot \sigma_1 \cdot t$, where g_{31} is the appropriate piezo stress constant, σ_1 is the longitude stress and t is the film thickness. Deflecting the PVDF film generates a strain gradient, which also results in an electric potential in direction 3, even when net strain is zero. The PVDF response is symmetric to deflection in both directions (not shown here).

III. Methods

A 3-D rapid-prototype machine (Objet Connex500) was employed to produce bi-bellow actuators (Fig. 3). The 3-D printer uses tiny droplets of resin to create a slice of the CAD model, cures this slice with UV light and then prints the next slice on top. Several types of resin can be used with various elastic moduli; the actuator's body has a Young modulus (E) of ∼0.45 MPa while the inlet and hoops are harder, E∼3.5 MPa (values of Young moduli, courtesy of Objet).

The internal cavity of each actuator is 7-mm in diameter and 120-mm long but the active length is slightly shorter, 104 mm (due to end-cap and inlet, see [12]). The body's external diameter is 10 mm and the cut-section second moment is ∼1000 mm^4. Rigid hoops were used to resist swelling of the rapid prototype models. Each hoop's diameter is Ø1 mm, and they are spaced along the bellows at a distance between centers of 4 mm.

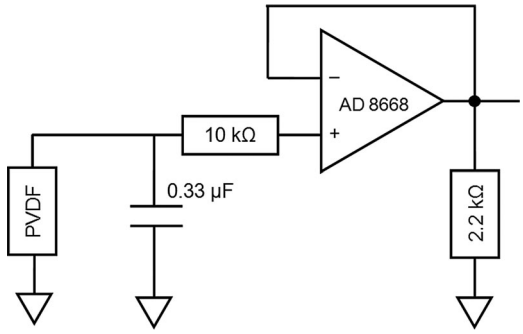

Fig. 4. Amplification scheme of PVDF signal.

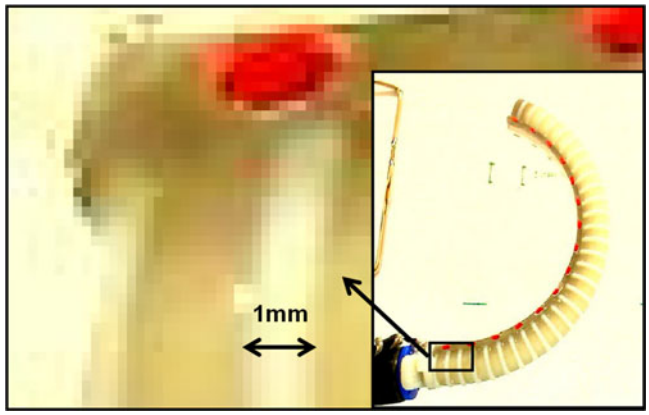

Fig. 5. Camera resolution.

The rigid inlet was used for anchoring the actuator. We installed an Intersema MS5407 pressure sensor to read the pressure at the inlet, relative to atmospheric pressure. The actuation pressure was monitored by a PI controller, implemented in LabVIEW as explained in [12]. PVDF strips 120-mm long, 4-mm wide and 52-μm thick were glued (Wacker Elastosil E41, silicone rubber) to the actuators' bottom side; facing the center of bending, so as not to inhibit deflection. The adhesive was applied to both sides of the PVDF and no delamination was detected. The PVDF tensile-stiffness (E = 2–4 GPa) is approximately 20-folds higher than that of the body of the bi- bellows, while the film's resistance to bending is practically nonexistent; attaching the PVDF actually enhances the bending action.

The PVDF voltage was read with a follow-amplifier circuit, schematically provided in Fig. 4. The capacitive PVDF sensor was connected in parallel to a capacitor of several orders of magnitude greater in order to lower the high-pass frequency beneath the working range, i.e., <0.1 Hz. PVDF readings were posttreated by removing the initial offset.

Fifteen visual tracers, 1.5-mm in diameter and 0.5-mm thick, were equally spaced along each side of the actuator. A USB camera (Logitech QuickCam Pro 9000, 2 Mega-Pixel) was used to photograph the actuator, where 1 pixel covers ∼1/8 mm × 1/8 mm as shown in Fig. 5. In postprocessing the markers' centroids were identified automatically by an algorithm specifically developed for this purpose, and the identification was then inspected by a user. Manual corrections were made when necessary on a small fraction of the frames. Typically, only a few of the 15 markers were misplaced on these problematic frames. The visual tracking facilitated the establishment of a ground truth for the actuator's shape during actuation. We demonstrate visual tracking of a single sinusoidal cycle in Fig. 6. The markers in each snap shot were

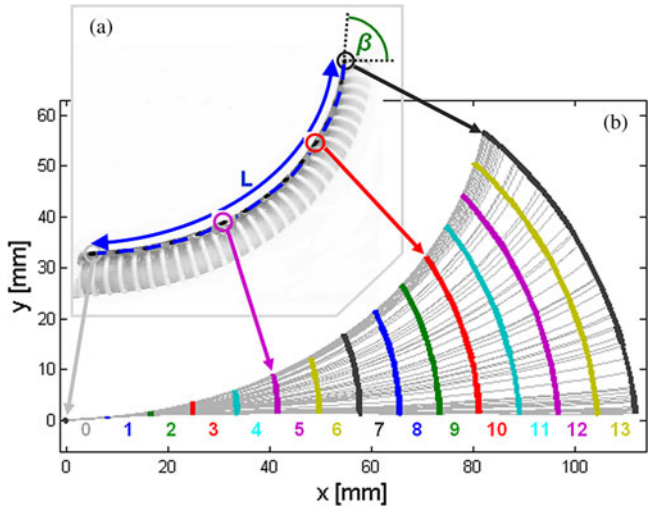

Fig. 6. Visual-tracking demonstration during a single cycle. (a) Snapshot with four tracers encircled, L—actuator length taken along a spline passing through the tracers, and β—the tip angle. (b) Tracer positions during the whole cycle are depicted by thick colored lines. A thin gray spline connects the tracers at each given point in time. The spline segments between each pair of tracers are numbered 0–13 and their length is recorded.

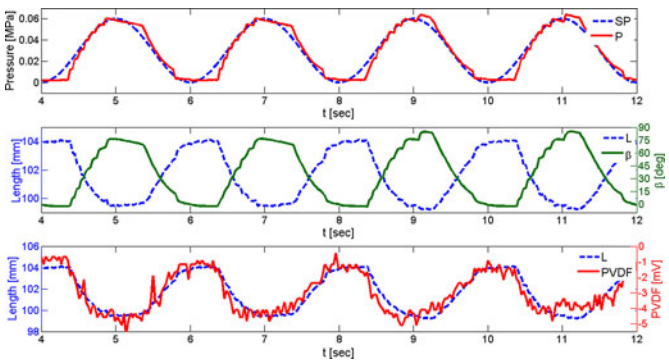

Fig. 7. Actuation trial of a free actuator bent up to 90°. Top—pressure set point (SP, dashed blue) versus the actual pressure measured (P, solid red). Middle—features extracted by visual tracking; actuator length (L, dashed blue), and tip angle (β, solid green). Bottom—PVDF reading (PVDF, solid red) versus the actuator length (L, dashed blue).

identified and their centers were traced. A cubic spline was generated through the tracer centers in each frame to estimate the actuator length.

IV. Results

We started by actuating a bi-bellows with a 0.5-Hz harmonic of 0.06 MPa (0.6 bar), i.e., a sine wave with a 0.03-MPa amplitude and a 0.03-MPa bias. Typical results can be seen in Fig. 7. The actuation pressure set point and the reading from the pressure sensor are displayed in the top axis. In the central axis, we show the tip angle (β) and the actuator length. We can see that β follows the actuation pressure, roughly linearly as reported in a previous work [12]. Contradictory to earlier reports, the length changes in the opposite phase to the actuation pressure. This behavior is easily explained by two facts.

1) The visual tracers sit "below" the neutral axis, on the inner side, which experiences competition between strain (causing elongation) and bending (inducing shortening).

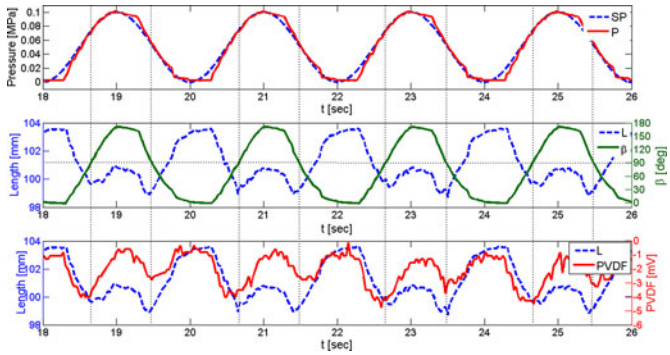

Fig. 8. Actuation trial of a free actuator bent up to 180°. Top—pressure set point (SP, dashed blue) versus the actual pressure measured (P, solid red). Middle—features extracted by visual tracking; actuator length (L, dashed blue), and tip angle (β, solid green). Bottom—PVDF reading (PVDF, solid red) versus the actuator length (L, dashed blue).

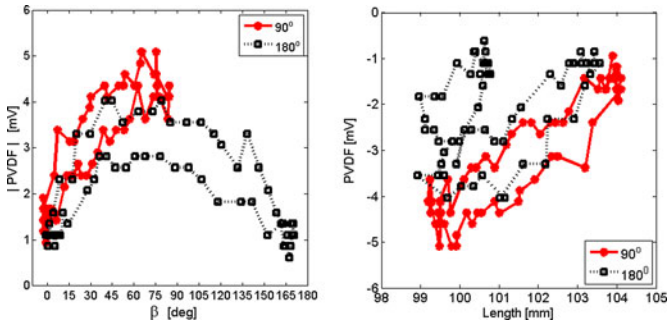

Fig. 9. Examples of PVDF response-loops in different work ranges. Left—PVDF (absolute values) versus deflection angle β. In the limited range ($\beta < 90°$) the PVDF monitors β well but, beyond this range, the PVDF loses any linear correlation to β. Right—examining the PVDF-length loops reveals that the PVDF signal resembles strain more than deflection outside the limited working range.

2) Attaching the PVDF strip to the bi-bellows yields a composite beam, which is much more resistant to tension than the bi-bellow itself, reducing net strain.

More interestingly, on the bottom axis of Fig. 7 we see that the PVDF follows the actuator's strain, accompanied by what seems to be a significant noise.

We repeated the experiment but this time with a 0.1 MPa or 1-bar harmonic (0.05-MPa amplitude + 0.05-MPa bias) which corresponds to a deflection angle of ∼180°. We noticed an unusual response (see Fig. 8, middle axis); while the tip's angle β adheres to the actuation pressure, the strain does not. Beyond a 90° tip angle (denoted by dotted lines), the tracers' fiber stops contracting and starts to stretch back to its original length. A possible reason for this phenomenon might be the exaggerated swelling, which increases the external diameter and reduces wall thickness, encouraging elongation over bending (see comments "1" and "2" on the previous page). However, this point is beyond our scope of interest. The PVDF response resembles the double-humped behavior of this geometric feature, as depicted in Fig. 8, bottom axis.

We examined the PVDF response loops in Fig. 9. The PVDF response follows both β and the actuator length L in the limited working range (<90°). In the larger working range (<180°), we noticed U-shaped response curves, in correlation to the double-humped profile we saw in Fig. 8. This information is summarized in Table I by examining the correlation ρ of the PVDF signal with the actuator length L,

TABLE I
PVDF SENSOR CORRELATIONS

Trial	Test	Feature	ρ	Pval
$\beta max = 90^0$	Pearson	L	0.92	< 1e-5
		β	-0.90	< 1e-5
		P	-0.95	< 1e-5
$\beta max = 180^0$	Spearman	L	0.47	< 2e-4
		β	0.05	insignificant
		P	-0.03	insignificant

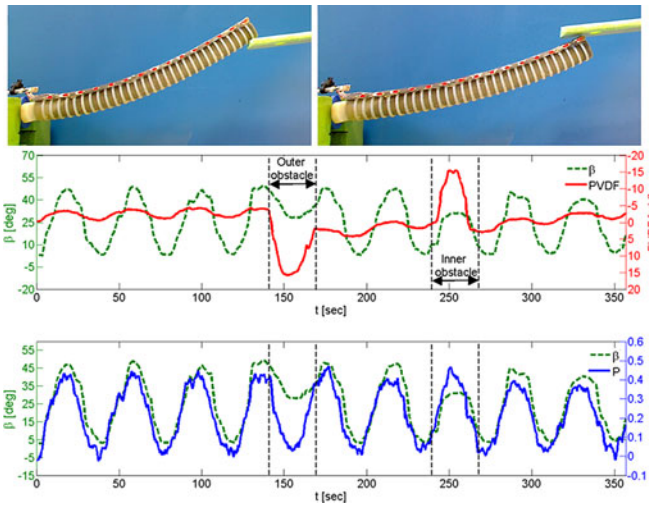

Fig. 10. Obstructed motion. The actuator was activated freely and then an obstacle was introduced. Top left—the external obstacle prevented the actuator from straightening during deflation. Top right—the inner obstacle stopped the actuator from bending during inflation. Both obstacles restricted the actuator to ∼30°. Middle—PVDF signal versus tip angle (β). Notice that the PVDF-axis is reversed. Bottom—reading from pressure sensor (P) versus β.

tip angle β and actuation pressure P during the single cycle used in Fig. 9.

After investigating free motion we proceeded to consider interactions with obstacles. In Fig. 10 we display how the actuator was obstructed during actuation, the tip's angle (β) versus the PVDF signal (top axis) and versus the pressure reading (P, bottom axis). The actuator was activated freely and then an outer obstacle was introduced, preventing straining. After a few free cycles, an internal obstacle was presented, restraining flexion. Again the PVDF followed the free motion, but contact with an obstacle stimulated a response of a higher magnitude. The pressure sensor remained indifferent to the kinematic constraint.

A rough calibration was conducted by holding the actuator at a slight angle, facing a force sensor (ATI Nano17) placed a few millimeters beneath its tip. For each measurement the actuation pressure was raised and held at some value for a short while, causing the bi-bellows to press down against the sensor. The force vector during contact consisted of normal and frictional components. We use ΔF to denote the force vector's norm and ΔPVDF for the difference in PVDF signal before and after contact. The results are displayed in Fig. 11, exhibiting roughly linear force sensing under the conditions mentioned.

It would be interesting to see what happens on a manipulator made of several segments, having a constraint applied to its distal link. Would the intermediate segments respond similarly to the free-motion behavior or to the constrained scenario?

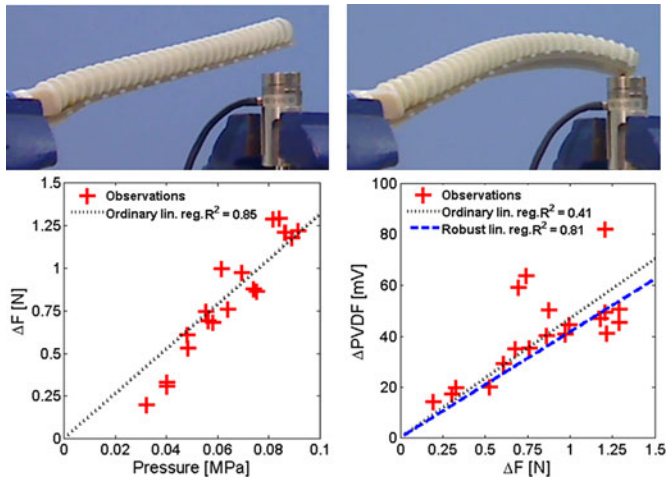

Fig. 11. Force-sensing calibration. Top left—initial free configuration. Top right—upon actuation the bi bellows presses against the force sensor. Bottom left—contact-force norm, ΔF, as a function of the actuation pressure. Bottom right—PVDF response, ΔPVDF, as a function of ΔF, the contact-force norm. Ordinary and robust linear-regression trend-lines are used.

V. CONCLUSION

Control of flexible actuators faces a fundamental difficulty; the significant influence of external forces and constraints on the actuator's shape. We propose a sensor integration solution, employing pressure and PVDF sensors. We demonstrated that the PVDF signal corresponds to a geometric feature (strain), independently of the actuation pressure. The PVDF corresponded to strain reasonably well in the 0–90° range but displayed a nonlinear response beyond the 90° limit. We will try to improve this problem by distributing several short sensors along the actuator instead of a single long strip. This is reminiscent of work done by Brett *et al.* [26] on a sensitized end effector, which is able to estimate the magnitude, location, and shape of external forces acting on a cantilever.

Operating at low frequencies, the PVDF signal suffers from poor SNR and drift—other circuits might be more suitable than the follow amplifier, e.g., a charge amplifier [20]. Overall, we conclude that the proposed sensor is able to monitor the shapes of bending actuators without inhibiting their operation. Further work is necessary to interpret the strain reading into shape.

Data fusion of PVDF and pressure sensors enables estimating of the location of the actuator tip and will be used for external force estimation and closed loop control. Combining several bi-bellow actuators will enable building stiffness-varying hyper-redundant robots for biomedical, biomimetic, and search and rescue applications.

REFERENCES

[1] G. S. Chirikjian, "Hyper-redundant manipulator dynamics: A continuum approximation," *Adv. Robot.*, vol. 9, pp. 217–243, 1994.
[2] Y. Muyari, Y. Haga, T. Mineta, and M. Esashi, "Development of hydraulic suction type active catheter using super elastic alloy tube," in *Tech. Dig. Sens. Symp.*, vol. 20, Tokyo, Japan, 2003, pp. 57–60.
[3] B. A. Jones and I. D. Walker, "Practical kinematics for real-time implementation of continuum robots," *IEEE Trans. Robot.*, vol. 22, no. 6, pp. 1087–1099, Dec. 2006.
[4] E. Tatlicioglu, I. D. Walker, and D. M. Dawson, "Dynamic modelling for planar extensible continuum robot manipulators," in *Proc. IEEE Int. Conf. Robot. Autom.*, Apr. 2007, pp. 1357–1362.
[5] K. Suzumori, S. Endo, T. Kanda, N. Kato, and H. Suzuki, "A bending pneumatic rubber actuator realizing soft-bodied manta swimming robot," in *Proc. IEEE Int. Conf. Robot. Autom.*, Apr. 2007, pp. 4975–4980.

[6] K. Xu and N Simaan, "An investigation of the intrinsic force sensing capabilities of continuum robots," *IEEE Trans. Robot.*, vol. 24, no. 3, pp. 576–587, Jun. 2008.

[7] K. Xu, R. E. Goldman, J. Ding, P. K. Allen, D. L. Fowler, and N. Simaan, "System design of an insertable robotic effector platform for single port access (SPA) surgery," in *Proc. IEEE/RSJ Int. Conf. Intell. Robots Syst.*, Oct. 2009, pp. 5546–5552.

[8] M. Ikeuchi and K. Ikuta, "Development of pressure-driven micro active catheter using membrane micro-emboss following excimer laser ablation (MeME-X) process," in *Proc. IEEE Int. Conf. Robot. Autom.*, Kobe, Japan, 2009, pp. 4358–4361.

[9] Y. Fu, H. Liu, W. Huang, S. Wang, and Z. Liang, "Steerable catheters in minimally invasive vascular surgery," *Int. J. Med. Robot.*, vol. 5, pp. 381–391, Dec. 2009.

[10] BionicTripod With FinGripper. Festo AG and Company. KG. Esslingen-Berkheim, Germany. (2009). [Online]. Available: http://www.festo.com/cms/en-ca_ca/10304.htm

[11] E. Brown, N. Rodenberg, J. Amend, A. Mozeika, E. Steltz, M. R. Zakin, H. Lipson, and H. M. Jaeger, "Universal robotic gripper based on the jamming of granular material [physics]," *Proc. Natl. Acad. Sci. USA*, vol. 107, pp. 18809–18814, 2010.

[12] Y. Shapiro, A. Wolf, and K. Gabor, "Bi-bellows: Pneumatic bending actuator," *Sensors Actuators A, Phys.*, vol. 167, no. 2, pp. 484–494, 2011.

[13] B. Gorissen, M. De Volder, A. De Greef, and D. Reynaerts, "Theoretical and experimental analysis of pneumatic balloon microactuators," *Sens. Actuators A, Phys.*, vol. 168, pp. 58–65, 2011.

[14] A. De Greef, P. Lambert, and A. Delchambre, "Towards flexible medical instruments: Review of flexible fluidic actuators," *Precis. Eng.*, vol. 33, no. 4, pp. 311–321, 2009.

[15] P. Manandhar, P. D. Calvert, and J. R. Buck, "An elastomeric ionic hydrogel sensor for large strains," in *Proc. IEEE 37th Annu. Northeast Bioeng. Conf.*, Apr. 2011, pp. 1–2.

[16] C. Mattmann, F. Clemens, and G. Tröster, "Sensor for measuring strain in textile," *Sensors*, vol. 8, pp. 3719–3732, 2008.

[17] T. Yamada, Y. Hayamizu, Y. Yamamoto, Y. Yomogida, A. Izadi-Najafabadi, D. N. Futaba, and K. Hata, "A stretchable carbon nanotube strain sensor for human-motion detection," *Nature Nanotechnol.*, vol. 6, pp. 296–301, 2011.

[18] Danfoss PolyPower A/S, Nordborg, Denmark, *PolyPower DEAP Technology for Actuators, Sensors and Energy Converters.* (2008). [Online]. Available: http://www.polypower.com/

[19] C. Li, P.-M. Wu, S. Lee, A. Gorton, M. J. Schulz, and C. H. Ahn, "Flexible dome and bump shape piezoelectric tactile sensors using PVDF-TrFE copolymer," *J. Microelectromech Syst.*, vol. 17, pp. 334–341, 2008.

[20] J. G. Webster and R. Pallás-Areny, "Signal conditioning for self-generating sensors," in *Sensors and Signal Conditioning*, 2nd ed., J. G. Webster and R. Pallás-Areny, Eds. New York: Wiley, 2001, pp. 375–432.

[21] Measurement Specialties. Hampton VA, *Piezo Film Sensors*, (2008). [Online]. Available: http://www.meas-spec.com/piezo-film-sensors.aspx

[22] W. Liu, A. Menciassi, S. Scapellato, P. Dario, and Y. Chen, "A biomimetic sensor for a crawling minirobot," *Robot. Autonom. Syst.*, vol. 54, no. 7, pp. 513–528, Jul. 31, 2006.

[23] Z. Chen, K. Kwon, and X. Tan, "Integrated IPMC/PVDF sensory actuator and its validation in feedback control," *Sens. Actuators A, Phys.*, vol. 144, pp. 231–241, 2008.

[24] K. Suzumori, S. Iikura, and H. Tanaka, "Applying a flexible microactuator to robotic mechanisms," *IEEE Control Syst. Mag.*, vol. 12, no. 1, pp. 21–27, Feb. 1992.

[25] Y. Yamamoto, K. Kure, T. Iwai, T. Kanda, and K. Suzumori, "Flexible displacement sensor using piezoelectric polymer for intelligent FMA," in *Proc. IEEE/RSJ Int. Conf. Intell. Robots Syst.*, Oct./Nov. 2007, pp. 765–770.

[26] P. N. Brett, "Smart sensing systems for surgical tool-points," in *Proc. 15th Int. Conf. Mechatron. Mach. Vis. Practice*, 2008, pp. 159–162.